Immunology & Cell Biology 2022; **100**: 250–266
www.wileyonlinelibrary.com/journal/icb

ORIGINAL ARTICLE

OPEN

The vaccinia-based Sementis Copenhagen Vector coronavirus disease 2019 vaccine induces broad and durable cellular and humoral immune responses

Preethi Eldi[1], Tamara H Cooper[1†], Natalie A Prow[1†], Liang Liu[1], Gary K Heinemann[1], Voueleng J Zhang[1], Abigail D Trinidad[1], Ruth Marian Guzman-Genuino[2], Peter Wulff[2], Leanne M Hobbs[1,2], Kerrilyn R Diener[1,3] & John D Hayball[1,2]

1 Experimental Therapeutics Laboratory, Clinical and Health Science Unit, University of South Australia, Adelaide, SA, Australia
2 Sementis Limited, Hackney, SA, Australia
3 Robinson Research Institute and Adelaide Medical School, The University of Adelaide, Adelaide, SA, Australia

Keywords
Antibodies, cellular responses, COVID-19, polyfunctional T cells, SARS-CoV-2, spike, vaccine

Correspondence
Preethi Eldi; Clinical and Health Sciences Unit, University of South Australia, GPO Box 2471, Adelaide, SA 5001, Australia.
Email: preethi.eldi@unisa.edu.au

John Hayball; Clinical and Health Sciences Unit, University of South Australia, GPO Box 2471, Adelaide, SA 5001, Australia.
Email: john.hayball@unisa.edu.au

Present address
Liang Liu, Gene Technologies Group, Department of Molecular Biology, CSL Limited, Parkville, VIC, Australia.

†Equal contributors.

Received 22 September 2021;
Revised 10 January and 15 February 2022;
Accepted 18 February 2022

doi: 10.1111/imcb.12539

Immunology & Cell Biology 2022; **100**: 250–266

Abstract

The ongoing coronavirus disease 2019 (COVID-19) pandemic perpetuated by severe acute respiratory syndrome coronavirus 2 (SARS-CoV-2) variants has highlighted the continued need for broadly protective vaccines that elicit robust and durable protection. Here, the vaccinia virus-based, replication-defective Sementis Copenhagen Vector (SCV) was used to develop a first-generation COVID-19 vaccine encoding the spike glycoprotein (SCV-S). Vaccination of mice rapidly induced polyfunctional CD8 T cells with cytotoxic activity and robust type 1 T helper-biased, spike-specific antibodies, which are significantly increased following a second vaccination, and contained neutralizing activity against the alpha and beta variants of concern. Longitudinal studies indicated that neutralizing antibody activity was maintained up to 9 months after vaccination in both young and middle-aged mice, with durable immune memory evident even in the presence of pre-existing vector immunity. Therefore, SCV-S vaccination has a positive immunogenicity profile, with potential to expand protection generated by current vaccines in a heterologous boost format and presents a solid basis for second-generation SCV-based COVID-19 vaccine candidates incorporating additional SARS-CoV-2 immunogens.

INTRODUCTION

Severe acute respiratory syndrome coronavirus 2 (SARS-CoV-2) responsible for coronavirus disease 2019 (COVID-19) was first detected in late 2019[1] in Wuhan (Hubei Province, People's Republic of China) and has since spread globally with 228 million confirmed cases and 4.69 million deaths as of September 2021.[2] Infection fatality rates are disproportionately high in aged individuals and individuals with comorbidities such as diabetes, cardiovascular diseases, obesity and immunosuppression.[3–6] The recent rapid spike in cases during the second and third waves of infection has been attributed to emerging variants of concern (VOCs) with reported increased transmissibility of

infection associated with changes across the viral genome, in particular the spike protein.[7–11] Although initial counter measures such as social distancing, masks and travel restrictions have played a major role in suppressing the spread, vaccines continue to be the most effective means to control severe illness and will play a major role in ending the enormous humanitarian and socioeconomic impact of the SARS-CoV-2 pandemic.

Currently, seven vaccines have been granted Emergency Use Listing by the World Health Organization, with a further 112 in clinical development and 185 in preclinical development using a wide array of technologies including nucleic acid-based vaccines,[12,13] replicating and nonreplicating viral vectored vaccines,[14–18] inactivated viruses[19,20] and protein subunit vaccines.[21] As a consequence of the unprecedented speed by which frontrunner vaccines were developed, there remains knowledge gaps in vaccine-mediated protection such as duration of protection, induction and relative importance of cell-mediated immunity, cross-protection against other coronaviruses and control of viral shedding and transmission. In addition, vaccines must meet the needs for rapid and successful deployment within the context of population-scale vaccination programs, with specific considerations given to large-scale manufacturability and distribution logistics. This highlights the need for continued COVID-19 vaccine development strategies using novel technologies that can build upon the successes of the frontrunner vaccines to provide robust, durable and broadly protective efficacy against variants as well as continue to address key logistical challenges.

The Sementis Copenhagen Vector (SCV) is a rationally designed, replication-defective viral vector technology based on the Copenhagen strain of vaccinia virus (VACV). Uniquely for a VACV-based vector, it has also been paired with a proprietary manufacturing cell line (MCL) to generate a platform system that can facilitate large-scale and tractable manufacturability of all SCV-based vaccines.[22] The SCV was generated by the targeted deletion of an essential viral assembly gene (*D13L*)[23,24] to prevent viral replication while retaining the powerful immunogenicity and large payload capacity of the parental virus. With sites B7R/B8R, C3L, A39R and A41L designated as antigen-insertion sites, it is also an ideal vector technology for multiantigen and multipathogen vaccines, such as the single-vectored dual chikungunya/Zika virus vaccine.[25] Systems vaccinology studies have demonstrated a localized type 1 T helper signature,[26] with advanced preclinical studies showing a fully attenuated and safe vaccine capable of inducing robust and long-lived antigen-specific antibody and CD8 T-cell responses equivalent to those elicited by replication competent VACV.[22] Efficacy of SCV vaccines has also been established in mouse and nonhuman primate challenge models of chikungunya and Zika virus infection.[22,25,27]

In this study, a first-generation SCV COVID-19 vaccine encoding the full-length, native spike glycoprotein (SCV-S) was constructed, with expression and cell surface anchorage of the spike protein in host cells confirmed. Detailed immunological analyses of vaccine-mediated immune responses demonstrated robust and long-lived spike-specific CD8 T-cell and neutralizing antibody responses in young and middle-aged mice, including inbred and outbred strains. Following a second booster dose, circulating neutralizing antibody levels were sustained without any discernible decay over a 9-month period. Assessment of long-lived CD8 T-cell and antibody-secreting cell compartments confirmed induction of durable spike-specific immune memory following vaccination. Therefore, this study presents evidence that SCV-based COVID-19 vaccines can mediate robust and durable serological and cellular priming which supports progression toward efficacy studies of second-generation vaccine candidates incorporating additional SARS-CoV-2 antigens, to build synergistic layers of additional protection.

RESULTS

Construction and characterization of an SCV expressing the SARS-CoV-2 spike protein

The proprietary SCV vaccine platform technology comprises (1) a VACV-based vector that is unable to produce infectious progeny through targeted deletion of an essential viral assembly protein (D13), which maintains amplification of the viral genome and late gene expression of introduced vaccine antigens for immune stimulation. This is combined with (2) an MCL based on Chinese hamster ovary (CHO) cells that constitutively express D13, for virion assembly, and CP77, an essential VACV host-range protein for CHO cells that provides replication capability for SCV vaccine production in suspension cultures using established commercial manufacturing technologies and facilities (Figure 1a).

To generate a spike encoding SCV vaccine (SCV-S), the unmodified full-length SARS-CoV-2 spike gene from the original Wuhan isolate-1 under the control of a synthetic VACV early/late promoter[28] was introduced by homologous recombination to replace the A41L open reading frame in SCV (Figure 1b). PCR analysis confirmed site-specific insertion of the heterologous SARS-CoV-2 spike sequence into SCV and absence of *D13L* (Figure 1c). Authentic expression of the spike protein was confirmed by infecting nonpermissive human 143B cells[22] with SCV-S or parent control vector (SCV containing no vaccine antigen) and detection of S1

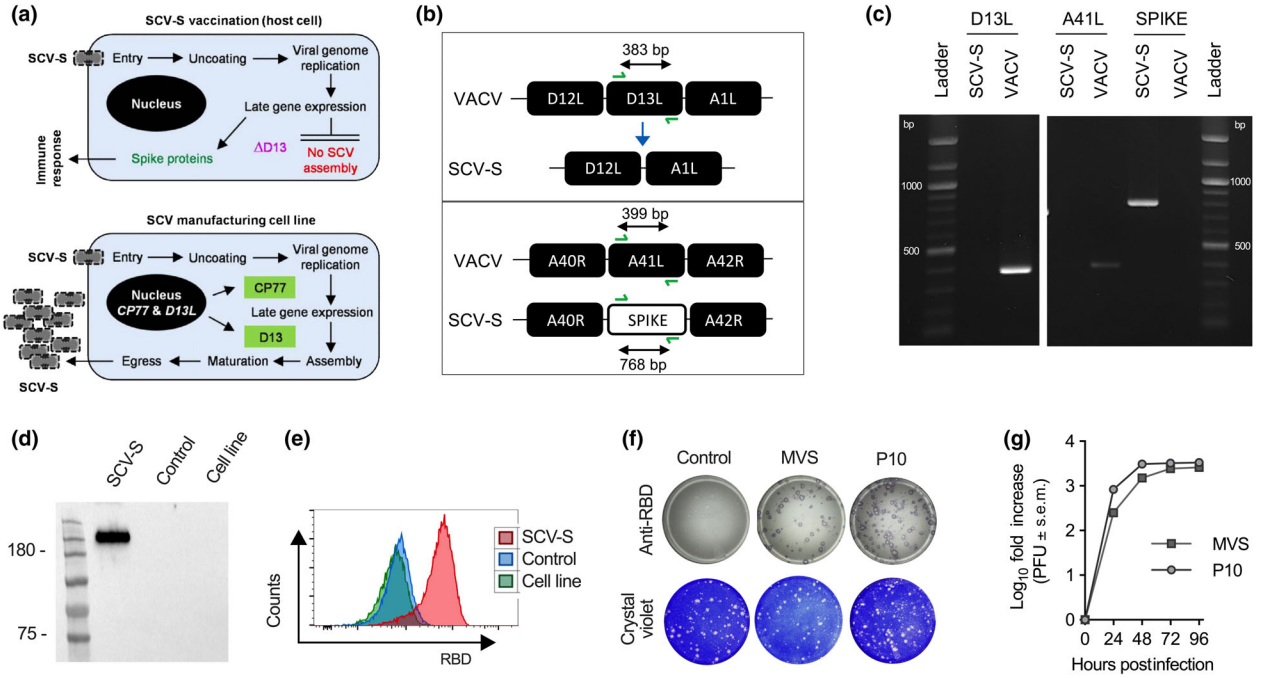

Figure 1. Vaccine construction and *in vitro* characterization. **(a)** Targeted deletion of *D13L* in SCV-S renders the viral vector unable to generate viral progeny by preventing virion assembly but allows for amplification of the SCV-S genome and late gene expression for production of spike protein to drive the vaccine-specific immune response (top panel). *In trans* provision of D13 and expression of the host range protein CP77 in the CHO-based manufacturing cell line allow for cell infection and rescue of virion assembly, allowing production of progeny for vaccine manufacture (bottom panel). **(b)** Schematic representation of SCV-S construction showing the *D13L* deletion and *A41L* substitution sites, with site-specific primers and the expected band size indicated. **(c)** Viral DNA from VACV and SCV-S was used for PCR analysis using the site-specific primers shown in **b** to confirm the deletion of D13L and insertion of spike. **(d)** Immunoblot analysis of spike antigen expression in SCV-S and control vector-infected 143B cells using an anti-S1 antibody. **(e)** Surface analysis of RBD expression in SCV-S or control vector-infected or uninfected MCL cells by flow cytometry using an anti-RBD antibody. **(f)** Immunostaining for RBD expression in STO1-33 cell monolayers infected with control vector, MVS or passage 10 (P10) stocks of SCV-S. Crystal violet was used to visualize plaques. **(g)** Manufacturing cell line was infected with MVS and P10 stocks of SCV-S vaccine at an MOI of 0.01 PFU, and viral titers were determined by plaque assay at the indicated times ($n = 3$ replicates). CHO, Chinese hamster ovary; MCL, manufacturing cell line; MOI, multiplicity of infection; MVS, master viral seed; PFU, plaque-forming units; RBD, receptor-binding domain; SCV-S, Sementis Copenhagen Vector spike protein; VACV, vaccinia virus.

production by immunoblot analysis (Figure 1d and Supplementary figure 1), as well as surface expression of the receptor-binding domain (RBD) in infected cells by flow cytometric analysis (Figure 1e).

The conversion of research-grade vaccine stock to cGMP-compliant master virus seed (MVS) and working virus seed stocks requires several passages, followed by subsequent expansion during manufacturing for large-scale SCV vaccine production. Therefore, the genetic stability of SCV-S was evaluated by serial passaging of the MVS up to 10 times (P10), which extends at least fivefold beyond the expected expansion requirement to reach commercial-scale vaccine batch production. Genetic integrity and sequence authenticity were confirmed by next-generation sequencing of MVS and P10 stocks (Supplementary figure 2). Immunostaining of MVS and P10 infected cell monolayers using anti-RBD antibody confirmed spike protein expression in all foci of viral infection (Figure 1f), with similar viral titer amplification ratios observed up to 72 h after infection (Figure 1g).

SCV-S vaccination stimulates rapid and functional cell-mediated immunity

The capacity of SCV-S to induce an early spike-specific cellular immune response was evaluated in C57BL/6J mice. One week after vaccination, splenocytes were stimulated with overlapping peptide pools spanning the S1 and S2 subunits of the SARS-CoV-2 spike protein and antigen-specific T-cell responses evaluated by interferon-γ (IFNγ) ELISPOT. Vaccination with SCV-S induced significant S1- and S2-specific IFNγ spot-forming units (SFUs) compared with mice vaccinated with control vector (Figure 2a). Consistent with the ELISPOT results, significantly elevated populations of S1- and S2-specific IFNγ-producing $CD8^+$ T cells were detected in

SCV-S-vaccinated mice compared with controls by intracellular cytokine staining (Figure 2b).

Effector CD8 T cells with cytotoxic potential produce granzyme B, a serine protease that is capable of mediating target cell lysis,[29] and a significant population of $CD8^+$ T cells were shown to express granzyme B in response to SCV-S vaccination (Figure 2c). To confirm cytotoxic activity, day 7 splenocytes were incubated with radiolabeled target cells pulsed with either S1 N-terminal domain (S1-NTD)-, RBD- or S2-specific peptide pools (Supplementary table 1). Significant cytolytic activity was detected against S1-NTD and RBD target cells (Figure 2d and Supplementary figure 3). The absence of functional activity against the S2 subunit suggested that the SCV-S vaccine primarily triggers an S1-specific cytotoxic T-cell profile. Together, these results indicated that the SCV-S vaccine induced an early expansion of spike-specific effector CD8 T cells with potential to reduce viral burden before the humoral arm of the immune response can be well established.

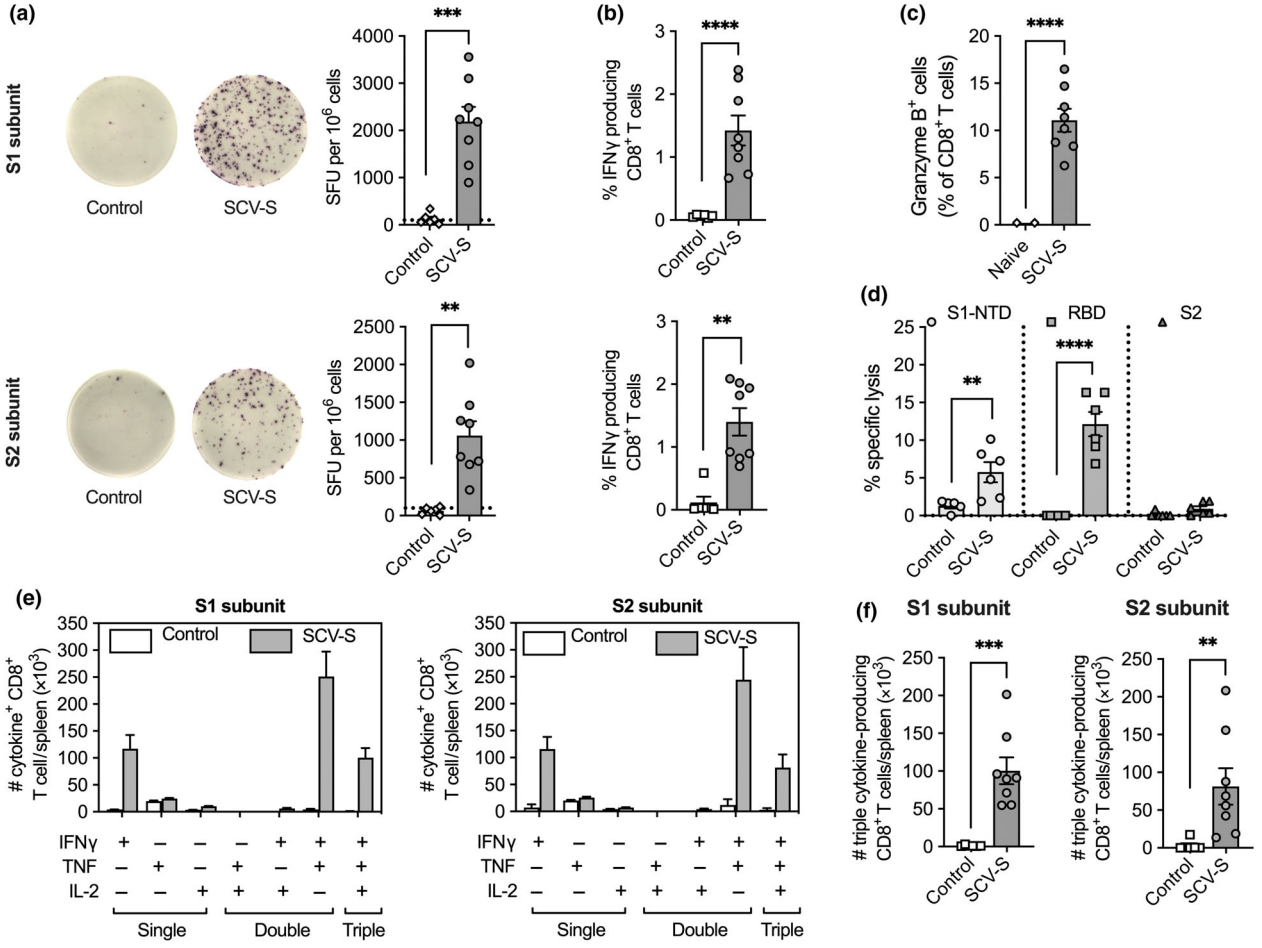

Figure 2. Early CD8 T-cell responses following SCV-S vaccination. Groups of C57BL/6J mice were vaccinated with 10^7 PFU of SCV-S or control vector and CD8 T-cell responses assessed 1 week later. **(a)** S1- and S2-specific IFNγ SFU quantitated by ELISPOT after stimulation of splenocytes with peptide pools (15-amino acid length with 11mer overlaps) spanning the S1 and S2 subunits of the spike protein. **(b)** Frequency of $IFN\gamma^+$ $CD8^+$ T cells specific for S1 and S2 subunit enumerated by intracellular cytokine staining. **(c)** Frequency of intracellular granzyme B^+ $CD8^+$ T cells in SCV-S-vaccinated or naïve controls. **(d)** Percentage specific lysis of MC57G target cells pulsed with S1-NTD-, RBD- and S2 subunit-specific peptides assessed by standard ^{51}Cr release *ex vivo* CTL assay. **(e)** Absolute number of single, double and triple cytokine-producing $CD8^+$ T cells in S1- and S2-stimulated splenocytes, with **(f)** S1- and S2-specific triple cytokine-producing CD8 T cells presented against that found in control vector groups. Analyses from one experiment conducted in equivalent numbers of male and female mice per group ($n = 6$ or 8/group) is depicted in **a**–**c**, **e** and **f**. Data in **a**, **b**, **e** and **f** are representative of a second independent experiment with similar results which was conducted in female mice ($n = 6$/group) to generate the data in **d**. Symbols represent individual mice and bars show the mean ± s.e.m. Data were log transformed and unpaired *t*-test with Welch's correction was used for statistical analysis. $^{**}P < 0.01$; $^{***}P < 0.001$; $^{****}P < 0.0001$. CTL, cytotoxic T lymphocyte; IFN, interferon; IL, interleukin; NTD, N-terminal domain; PFU, plaque-forming units; RBD, receptor-binding domain; SCV-S, Sementis Copenhagen Vector spike protein; SFU, spot-forming units; TNF, tumor necrosis factor.

Previous studies have demonstrated that CD8 T cells that produce multiple cytokines have enhanced effector functions and support maturation of an antigen-specific memory T-cell population.[30,31] Therefore, S1- and S2-specific cytokine producing $CD8^+$ T cells were profiled into seven distinct populations based on the production of IFNγ, tumor necrosis factor (TNF), interleukin-2 (IL-2) and their combinations (Supplementary figure 4). Polyfunctional $IFN\gamma^+$ TNF^+ cells dominated the responding S1- and S2- specific T-cell population, followed by $IFN\gamma^+$ TNF^+ $IL\text{-}2^+$ (triple cytokine producing) and single $IFN\gamma^+$ producing cell population (Figure 2e). Furthermore, significant numbers of S1- and S2-specific triple cytokine-producing $CD8^+$ T cells (Figure 2f), produced more cytokines on a per-cell basis than double and single cytokine-producing $CD8^+$ T cells (Supplementary figure 5).

SCV-S vaccination induces spike-specific binding and neutralizing antibody responses

Immunogenicity of SCV-S was evaluated in C57BL/6J mice, with kinetics of spike-binding antibody responses assessed up to day 28 after vaccination. S1 and S2 immunoglobulin M (IgM)-binding titers peaked at day 7 after vaccination and then returned to baseline levels by day 20 (Figure 3a; top panels). Class-switched S1 IgG-binding titers were detected in all mice by day 9 after vaccination, with the appearance of S2 IgG-binding antibodies delayed to days 15–19 after vaccination (Figure 3a, lower panels). The World Health Organization target product profile for COVID-19 vaccines[32] and current understandings in the field indicate that a type 1 T helper-biased humoral and cellular immune responses is required to prevent vaccine-associated enhanced respiratory disease.[33,34] Subclass profiling of day 28 postvaccination serum samples revealed a strong IgG2c response with an associated IgG2c-to-IgG1 ratio of >1 confirming a type 1 T helper-biased spike-specific antibody response (Figure 3b and Supplementary figure 6).

Outbred strains of mice are more representative of the genetic variability in the general human population and therefore the dominant S1-binding antibody responses in inbred and outbred strains of mice were compared at day 21 after vaccination. S1 IgG-binding titers were comparable between the two strains of mice, were significantly higher than the controls and translated into significant levels of neutralizing activity (Figure 3c).

To understand the long-term kinetics of the spike-specific antibody response, serum samples from outbred ARC(s) mice were evaluated up to 6 months after vaccination. S1-binding titers remained significantly elevated compared with naïve mice at all timepoints tested, although a trend in reduced titer was observed from 3 months. Significant neutralizing activity was also maintained, albeit with a small steady decline after 3 months (Figure 3d). A similar trend was observed in C57BL/6J mice, with significant S1-specific antibody-binding titers and neutralizing activity maintained up to 12 weeks after vaccination, although neutralization activity had halved between 3 and 12 weeks (Supplementary figure 7). Therefore, to stabilize the waning antibody responses, a 4-week homologous prime/boost vaccination strategy was assessed in C57BL/6J mice. At 3 weeks after the boost, a significant increase in both S1 IgG-binding titers and neutralizing activity was detected in the prime-boost cohort compared with single-dose and control vector-vaccinated mice (Figure 3e). A positive correlation between the S1-specific IgG-binding titers and neutralization activity was confirmed (Supplementary figure 8).

Given the emergence of SARS-CoV-2 variants that can exhibit increased replicative and transmission fitness, the SCV-S vaccine-generated neutralization antibody response was assessed against the recognized alpha and beta VOCs. First, the capacity to block the interaction between viral RBD and the host angiotensin-converting enzyme 2 (ACE2) receptor was assayed using the RBD protein from the original Wuhan isolate-1, N501Y alpha VOC or the E484K, K417N and N501Y beta VOC. All serum samples inhibited the binding between the ACE2 receptor and the RBD from the original Wuhan isolate-1, with a 1.1- and 2.1-fold reduction in inhibition detected for the alpha and beta VOCs (Figure 3f). Next, using SARS-CoV-2-pseudotyped lentiviruses containing the spike sequence of either the Wuhan isolate-1, alpha or beta VOCs, the effect of mutations on the serum neutralizing capacity was examined. A similar result, with a significant 3.2- and 4.1-fold reduction in the 80% inhibitory concentration, was noted for the alpha and beta VOCs compared with the original Wuhan isolate-1 (Figure 3g).

The persistence of neutralizing antibody responses is important in all populations, including the aging population. Therefore, the durability of the SCV-S induced neutralizing activity was evaluated in both young (6–8-week old) and middle-aged (9–10-month old) mice. S1-binding (Supplementary figure 9) and functional neutralizing antibodies (Figure 3h) were maintained without any significant decrease in titer up to the termination of the study at 3 months after boost vaccination. Importantly, no significant differences were detected in the neutralizing capacity between the young and middle-aged mice. In summary, these results indicate that prime-boost vaccination with SCV-S induces a robust and durable spike-specific antibody response with neutralizing capacity against the original Wuhan isolate-1, and both alpha and beta VOCs.

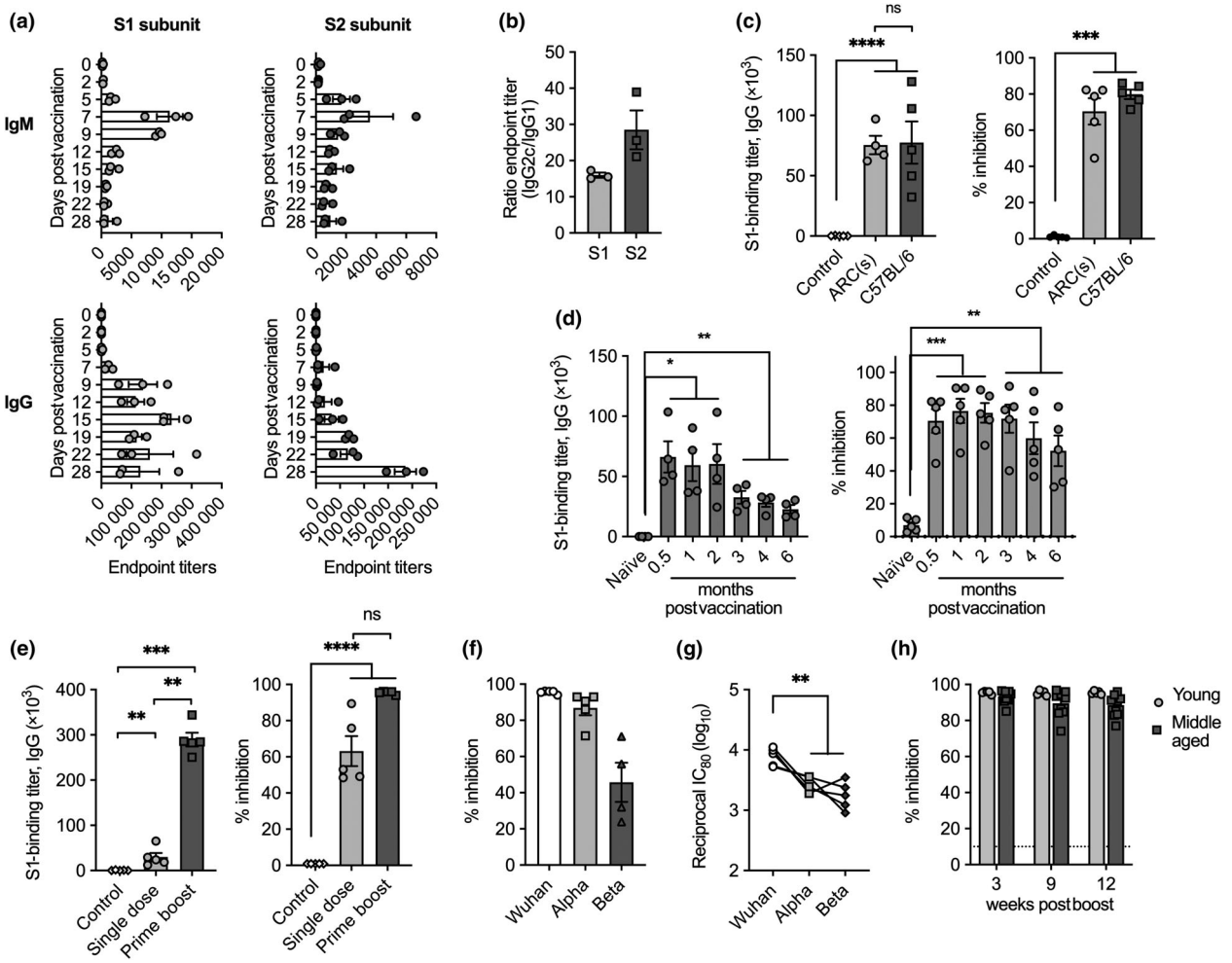

Figure 3. Spike-specific antibody and SARS-CoV-2 neutralization responses following SCV-S vaccination. **(a)** S1 and S2 subunit endpoint IgM and IgG ELISA titers determined from serum of female C57BL/6J mice (n = 3) at the indicated times after a single vaccination with 10^7 PFU of SCV-S, with **(b)** ratio of S1- and S2-specific IgG2c to IgG1 endpoint ELISA titers determined 28 days after vaccination. **(c)** S1 IgG ELISA binding titers (left panel) and cPass neutralization titers (right panel) in outbred ARC(s) and inbred C57BL/6J female mice (n = 5) 21 days after a single vaccination with 10^7 PFU of SCV-S or vector control, with **(d)** durability of response in the outbred cohort shown by S1-specific endpoint IgG ELISA titers (left panel) and neutralization titers (right panel) at the indicated times. **(e)** S1-specific IgG ELISA (left panel) and neutralization titers (right panel) 50 days after a single-dose (day 0) or prime-boost (day 0 and 28) vaccination of female C57BL/6J mice (n = 5) with 10^7 PFU SCV-S or control vector, with **(f)** neutralizing activity in ACE2 and RBD blocking ELISA, and **(g)** neutralizing activity (IC_{80} titers) against lenti-SARS-CoV-2-S pseudoviruses bearing spike protein from the Wuhan reference strain, the alpha or beta variant, shown for prime-boost samples. **(h)** Neutralization titers in young (6–8 weeks old; n = 5) and middle-aged (9–10 months old; n = 10) C57BL/6J mice at the indicated times after prime-boost vaccination with 10^7 PFU SCV-S. Results shown are representative of four independent experiments (indicated above) with binding and neutralizing antibody levels comparable at similar doses and time points across all experiments. Symbols represent individual mice and bars show the mean ± s.e.m. from independent experiments. Data were log transformed and statistical significance determined using Brown–Forsythe and Welch ANOVA with Dunnett T3 multiple comparison test. *$P < 0.05$; **$P < 0.01$; *** $P < 0.001$; ****$P < 0.0001$. ACE2, angiotensin-converting enzyme-2; IC_{80}, 80% inhibitory concentration; Ig, immunoglobulin; ns, not significant; PFU, plaque-forming units; RBD, receptor-binding domain; SARS-CoV-2, severe acute respiratory syndrome coronavirus 2; SCV-S, Sementis Copenhagen Vector spike protein.

Prime-boost vaccination with SCV-S enhances antigen-specific memory T-cell responses

To examine SCV-S-induced cellular immune responses, C57BL/6J mice were immunized in a single dose (day 0) or prime-boost (day 0 and 28) vaccination protocol, with spike-specific memory $CD8^+$ T-cell populations studied 3 months later. Mice vaccinated with control vector in a prime-boost strategy were used as appropriate controls. Following a single dose of the vaccine, S1-NTD-specific $IFN\gamma^+$ SFU were detected above the background determined by control vector-vaccinated mice; however, a

significant 4.3-fold increase over controls was noted with a prime-boost regimen (Figure 4a). This correlated with an increased frequency of IFNγ^+-producing CD8$^+$ T cells and absolute numbers of polyfunctional IFNγ^+ TNF$^+$ IL-2$^+$-expressing CD8$^+$ T cells, with the prime-boost regimen significantly elevating the response over that detected in single dose and control-vaccinated mice (Figure 4b). A similar significant increase in RBD-specific and S2-specific IFNγ^+ SFU and IFNγ-expressing and polyfunctional CD8$^+$ T cells was noted in the prime-boost-vaccinated mice compared with the single dose and control-vaccinated mice; however, a single dose also induced a significant population of RBD-specific and S2-specific IFNγ^+ CD8$^+$ T cells and triple cytokine-producing cells (Figure 4c–f).

Analysis of the total spike-specific CD8$^+$ T-cell IFNγ^+ responses revealed an immunodominance of RBD-specific responses, with about 65% of the total spike-specific responses targeting the RBD region of the spike protein. Further cytokine profiling of this RBD-specific CD8$^+$ T-cell population revealed that the prime-boost vaccination regimen significantly increased the mean frequency of multifunctional T cells from 32% with a single dose to 80% with a prime boost. This consisted of an average 3.3-fold increase in double-positive, and 1.7-fold increase in triple-cytokine positive cells compared with single-dose-vaccinated mice (Figure 4g, h). Similar trends were observed in middle-aged mice, with prime-boost vaccination inducing significantly higher S1-NTD-, RBD- and S2-specific IFNγ-producing cells than in single-dose and control-vaccinated mice (Supplementary figure 10).

Vector-specific memory T-cell responses were also assessed. As expected, prime-boost SCV-S and control vector-vaccinated mice had significantly higher levels of vector-specific IFNγ SFU, IFNγ^+ CD8$^+$ T cells and triple cytokine-positive cells, than single-dose-vaccinated mice (Supplementary figure 11). Overall, prime-boost vaccination significantly increased the CD8$^+$ short-lived effector T-cell and long-lived effector memory T-cell populations in general. No significant changes were observed in the central memory T-cell compartment (Supplementary figure 12). Altogether, these results confirm that prime-boost vaccination with SCV-S enhances the spike-specific memory CD8$^+$ T-cell response in both young and middle-aged populations of mice.

Pre-existing vector immunity constrains the magnitude of cellular immune responses, but has no impact on spike-specific humoral immune responses

The presence of VACV-specific memory immune responses, particularly in a small cohort of the aged population that had previously received a smallpox vaccination, may impact on the induction of vaccine antigen-specific cellular and humoral immune responses from recombinant SCV vaccines. A mouse model of robust pre-existing vector immunity was established to study its impact on spike-specific immune responses following vaccination with SCV-S. Mice were administered a single dose of replicative VACV, with presence of vector-specific antibody responses confirmed 6 weeks later (Figure 5a). After 8 weeks, mice were vaccinated with SCV-S vaccine in a 4-week prime-boost strategy, and the magnitude and quality of spike-specific antibody and T-cell responses were evaluated. Naïve mice were used as controls for vector-specific immune responses and mice vaccinated with control vector were used as controls for antigen-specific responses. Two weeks after the SCV-S booster dose administration, no significant differences in S1- and S2-specific IgG-binding titers between cohorts with (+) or without (−) pre-existing immunity were observed (Figure 5b). Consistent with the binding titers, SARS-CoV-2 neutralization activity was comparable between the two groups of mice (Figure 5c). Importantly, neutralizing activity was not impacted by pre-existing immunity even at 3 months after SCV-S vaccination (Figure 5d).

Next, the impact of pre-existing immunity on spike-specific memory CD8 T-cell responses at 3 months after SCV-S vaccination was evaluated in the spleen using peptide pools specific to S1-NTD, RBD and S2 regions of the spike protein. As anticipated, irrespective of the pre-existing immunity status, SCV-S-vaccinated mice had significantly higher S1-NTD-, RBD- and S2-specific IFNγ^+ SFU than control-vaccinated mice (Figure 5e). However, approximately 10–15-fold lower S1-NTD- and RBD-specific T-cell responses were noted in mice with pre-existing VACV memory responses than in VACV naïve mice, suggesting that the magnitude of the spike-specific T-cell responses was impacted on by pre-existing vector immunity. Assessment of the IFNγ^+ CD8$^+$ T-cell population confirmed a 20-fold increase in IFNγ expression in response to SCV-S prime-boost vaccination in VACV naïve mice compared with VACV-experienced cohorts (Figure 5f).

Further analysis of the dominant RBD-specific CD8$^+$ T-cell responses revealed a higher proportion of RBD-specific multifunctional T cells in VACV naïve mice than in VACV-experienced mice, with a specific increase in IFNγ^+ cells co-expressing TNF (Figure 5g). Despite a lower proportion of multifunctional T cells within the cytokine-producing CD8$^+$ T cells, significant numbers of RBD-specific triple cytokine-positive cells in VACV-experienced mice could still be detected compared with control-vaccinated mice (Figure 5h). Together, this indicated that pre-existing vector immunity had no significant effect on the humoral immune response, and while this significantly reduced the magnitude of the

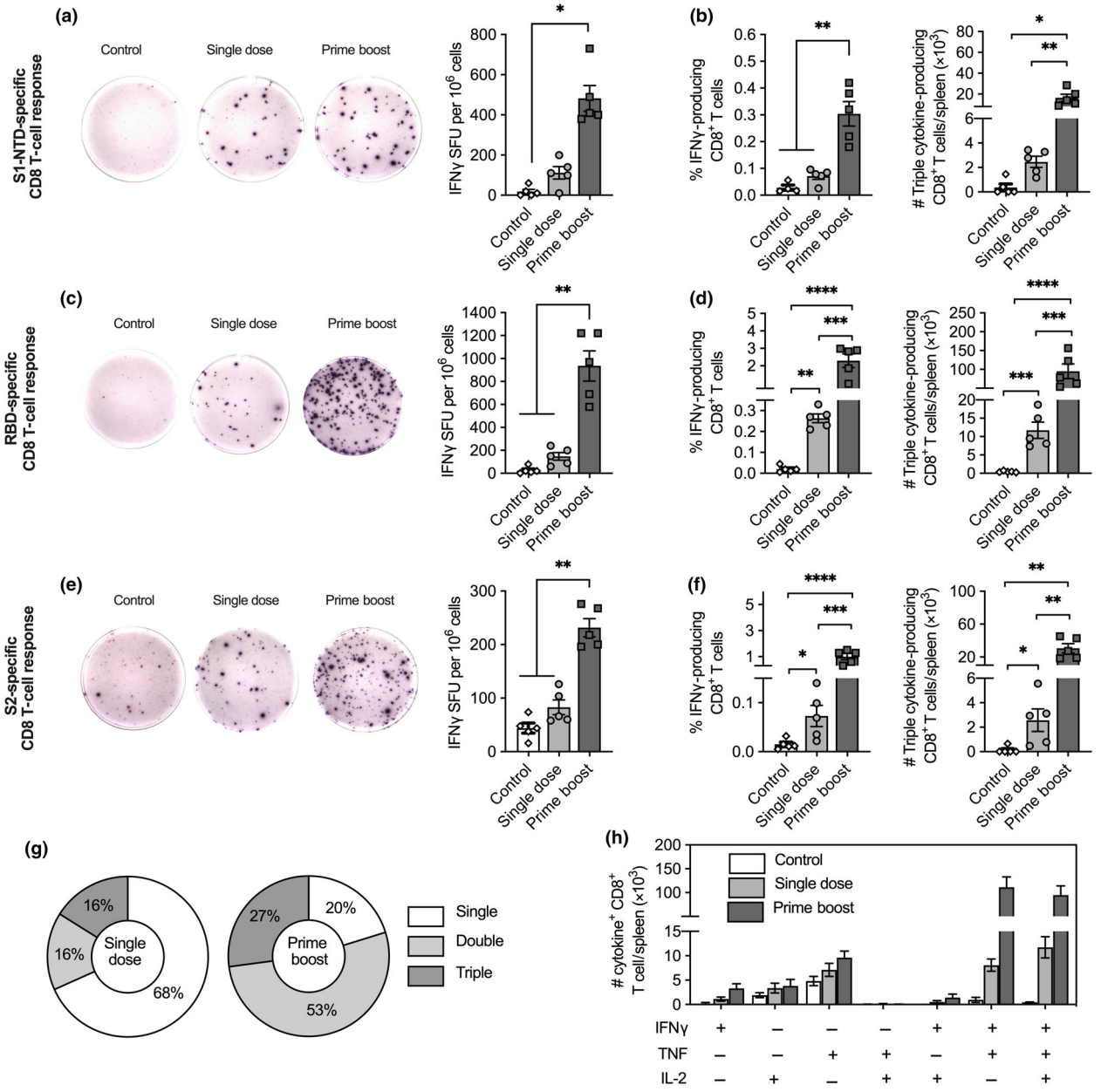

Figure 4. Spike-specific CD8 T-cell responses 3 months after SCV-S vaccination. Groups of female C57BL/6J mice (n = 5) were vaccinated in a single dose (day 0) or prime-boost strategy (day 0 and 28) with 10^7 PFU SCV-S. Mice vaccinated with control vector on days 0 and 28 were used as controls. At day 120, splenocytes were stimulated with peptide pools (15-amino acid length with 11mer overlaps) spanning the spike protein to examine antigen-specific T-cell responses. **(a, c, e)** IFNγ SFU specific for S1-NTD, RBD- and S2-specific subunit regions of the spike protein was quantitated by ELISPOT. **(b, d, f)** Corresponding frequency of IFNγ$^+$ CD8$^+$ T cells and absolute numbers of triple cytokine (IFNγ$^+$ TNF$^+$ IL-2$^+$) producing CD8 T cells as enumerated by intracellular cytokine staining and FACS analysis. **(g)** Graphs showing the mean frequency and **(h)** absolute numbers of RBD-specific single (IFNγ$^+$, TNF$^+$ or IL-2$^+$), double (TNF$^+$ IL-2$^+$, IFNγ$^+$ IL-2$^+$ or IFNγ$^+$ TNF$^+$) and triple cytokine (IFNγ$^+$ TNF$^+$ IL-2$^+$) cells within the cytokine-positive CD8 T-cell compartment. Results from single-dose cohorts are representative of similar results obtained from independent assessment of inbred and outbred strains of mice at 6 months of age (Figure 3c, d and Supplementary figure 7). Results from prime/boost cohorts are representative of those obtained in independent experiments depicted in Figure 5. Symbols represent individual mice and bars show the mean ± s.e.m. from one experiment. Data were log transformed and statistical significance determined using Brown–Forsythe and Welch ANOVA with Dunnett T3 multiple comparison test. *P < 0.05; **P < 0.01; ***P < 0.001; ****P < 0.0001. IFN, interferon; IL, interleukin; NTD, N-terminal domain; PFU, plaque-forming units; RBD, receptor-binding domain; SCV-S, Sementis Copenhagen Vector spike protein; SFU, spot-forming unit; TNF, tumor necrosis factor.

spike-specific memory $CD8^+$ T-cell response, vaccination with SCV-S could still, however, induce significant spike-specific cellular responses.

Middle-aged mice demonstrate long-lived and robust spike-specific cellular and humoral immune responses following SCV-S vaccination

Long-lived immunological memory forms the basis of robust prevention of disease following vaccination. Previous studies have demonstrated that impaired immune responses in older individuals can be associated with decreased immunological memory after vaccination.[35,36] Therefore, the ability of SCV-S to establish a long-lived spike-specific immune response was investigated. Young and middle-aged C57BL/6J mice were vaccinated in a 4-week prime-boost regimen, and spike-specific immune responses were analyzed 9 months after vaccination. Significant S1-binding IgG titers were observed in both young and middle-aged mice compared with control-vaccinated mice, with no statistical difference observed between the groups (Figure 6a, left panel). Surprisingly, S2-binding titers were detected only in four out of five middle-aged mice, and while the mean S2 IgG-binding titers in the middle-aged mice were higher than the control-vaccinated mice, it was not statistically different. The young mice, by contrast, had significant S2 IgG-binding titers compared with the control-vaccinated mice (Figure 6a; right panel). Retrospective analysis of the S2-binding titers in the young and middle-aged mice during the vaccination time course revealed that the levels were comparable at day 21 after prime; however, no further increase in the S2-binding titers in middle-aged mice followed the booster dose. In comparison, an approximate 10-fold increase in the S2-binding titers were detected in young mice after boost vaccination (Supplementary figure 13). Despite these differences in the S2-binding titers, the neutralization activity was comparable between the young and middle-aged mice at 9 months (Figure 6b). Persistent antigen-specific antibody levels in the serum are maintained by long-lived antibody-secreting cells that reside in the bone marrow.[37,38] Both the young and middle-aged mice demonstrated significant numbers of S1-specific antibody-secreting cells compared with the control-vaccinated mice, with the populations comparable between the two groups (Figure 6c).

Consistent with the antibody responses, spike-specific T-cell responses were maintained in both young and middle-aged mice at 9 months after vaccination. Significant numbers of S1-NTD- (Figure 6d), RBD- (Figure 6e) and S2- (Figure 6f) specific $IFN\gamma^+$ SFU and $IFN\gamma^+$ $CD8^+$ T cells were detected in both the young and middle-aged mice compared with the control-vaccinated mice, with no statistical difference noted between the two groups. The proportions of multifunctional T cells within the cytokine-producing $CD8^+$ T-cell population across all three regions of the spike protein were also comparable (Supplementary figure 14). Triple cytokine-producing $CD8^+$ T cells that have enhanced cytokine and memory potential were also detected in significant numbers in all groups except S2-targeting triple cytokine-producing $CD8^+$ T cells, which suggested that S1-specific polyfunctional effector cellular responses dominate the memory compartment following SCV-S vaccination. In summary, these results indicate that SCV-S vaccination induces a long-lived humoral and cellular immunity, with similar magnitude and quality of immune responses in both young and middle-aged mice, demonstrating broad applicability of SCV-S.

DISCUSSION

Vaccine development programs that enhance existing vaccine technologies and advance development of novel vaccine platforms are critical in the current race to curb SARS-CoV-2 evolution and control the COVID-19 pandemic. Complementary and synergistic vaccination strategies and cohort-specific vaccination approaches are rapidly gaining acceptance, because of a lack of effective antiviral therapies, a broad range of vulnerable populations and the intrinsic manufacturing challenges associated with global vaccination campaigns. In the current stage of the pandemic, a potential vaccine candidate should satisfy one or more of the following criteria: induce a broad and robust humoral and cellular immune response against the dominant circulating variants, establish long-lived immune responses that can maintain herd immunity and prevent circulation of SARS-CoV-2 and variants, provide cross-protection against other coronaviruses and have a stream-lined and tractable manufacturing process.

The SCV vaccine platform technology builds on the favorable characteristics of the parental VACV vector, namely, long-lasting cellular and humoral immune responses, significant antigen payload capacity and cold-chain-independent vaccine distribution capability, and incorporates additional advantages, primarily safety while maintaining immunogenicity. SCV-based vaccines have proven stability at 4°C for 6 months in simple salt-buffered liquid formulations, and at least 1 year in dried formulations (unpublished data), which may address the logistical difficulties associated with vaccine deployment in hard-to-reach and vulnerable communities. Furthermore, the SCV platform addresses the manufacturing challenges associated with the use of primary cells in empirically attenuated VACV-based vaccine production; industry-standard CHO cells were uniquely genetically engineered

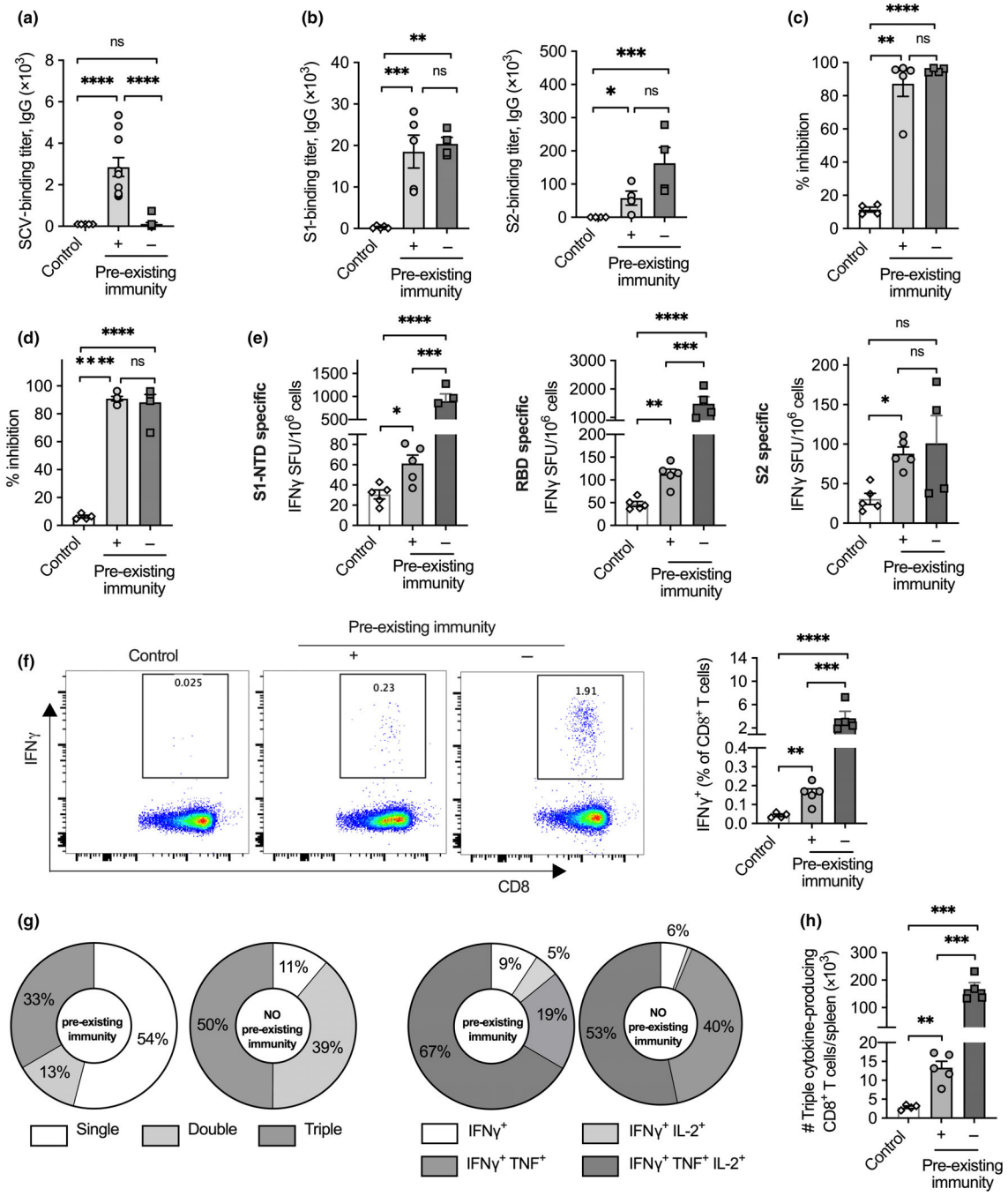

to allow high-yield production of SCV vaccines. This study describes the immunogenicity of a first-generation SCV-mediated COVID-19 vaccine incorporating the SARS-CoV-2 spike glycoprotein, which mediates viral attachment and entry into host cells. The data presented here show that SCV-S-infected cells produce the spike immunogen that is transported to the cell surface to stimulate antigen-specific immune responses. Importantly, the spike insert was maintained in the viral genome without any loss or changes in transgene sequence or protein expression, thus confirming the genetic stability of the vaccine through several passages, which is an inherent characteristic to support large-scale vaccines manufacturing protocols.

Immunogenicity studies in mice confirmed that the vaccine induces spike-specific functional T-cell responses in 1 week, and robust levels of circulating spike-specific

Figure 5. Impact of pre-existing vector immunity on spike-specific antibody and CD8 T-cell responses. Cohorts of C57BL/6J mice containing both genders ($n = 5$ in total) were vaccinated at day −60 with VACV at 10^5 PFU or diluent only to generate groups with and without pre-existing immunity. Mice were subsequently vaccinated with 10^7 PFU SCV-S at day 0 and 28. **(a)** Vector-specific endpoint IgG ELISA titers 28 days after exposure to VACV or diluent control. **(b)** S1 (right panel) and S2 (left panel) IgG ELISA, and **(c)** neutralization titers 50 days after vaccination. **(d)** Maintenance of neutralization activity 3 months after vaccination. **(e)** S1-NTD-, RBD- and S2-specific IFNγ SFU were quantitated by ELISPOT in splenocyte populations stimulated with peptide pools (15-amino acid length with 11mer overlaps) spanning the spike protein 90 days after vaccination. **(f)** Intracellular cytokine staining and FACS analysis showing frequency of $IFN\gamma^+$ $CD8^+$ T cells specific for the RBD region of the spike protein. **(g)** Pie charts comparing the mean proportions of single, double and triple cytokine-producing cells (left panels) and frequency of multifunctional IFNγ-producing T-cell populations (right panels). **(h)** Absolute numbers of RBD-specific triple cytokine ($IFN\gamma^+$ TNF^+ $IL\text{-}2^+$) cells within the cytokine-positive CD8 T-cell compartment. Results from cohorts with no pre-existing immunity are representative of similar antibody and T-cell results obtained at similar time points from independent prime-boost experiments depicted in Figures 3 and 4, respectively. Symbols represent individual mice and bars show the mean ± s.e.m. from one experiment. Data were log transformed and statistical significance determined using Brown–Forsythe and Welch ANOVA with Dunnett T3 multiple comparison test. $*P < 0.05$; $**P < 0.01$; $***P < 0.001$; $****P < 0.0001$. FACS, fluorescence-activated cell sorting; IFN, interferon; Ig, immunoglobulin; IL, interleukin; NTD, N-terminal domain; PFU, plaque-forming units; RBD, receptor-binding domain; SCV-S, Sementis Copenhagen Vector spike protein; SFU, spot-forming unit; TNF, tumor necrosis factor; VACV, vaccinia virus.

antibodies in both inbred and outbred strains of mice, with significant neutralizing activity detected within 2 weeks of vaccination. These functional immune responses satisfy the rapid onset of protection criteria set forth in the COVID-19 vaccine target product profile by the World Health Organization, a promising attribute for a stand-alone vaccine in establishing ring immunity and preventing spread of infection. While a direct comparison of the neutralizing activity with other frontrunner vaccines would be useful, differing protocols and analyses used across diverse vaccine platforms deployed and in development make it virtually impossible to do so. Instead, neutralizing activity against SARS-CoV-2 and the VOCs (alpha and beta) was confirmed by two different methods: (1) using an FDA-approved validation methodology[39] that detects antibodies that block the interaction between RBD (and variants thereof) and the ACE2 cell surface receptor, and (2) a lentiviral-based pseudovirus neutralization assay. Importantly, after two doses the circulating neutralizing antibody responses were maintained long term with minimal contraction, up to 9 months after vaccination, in both young and middle-aged mice. With a clear aim to provide a detailed immunological analysis of the SCV-S vaccine, particularly durability of responses, we used 9–10-month-old middle-aged mice that could then be assessed at least 9 months after vaccination (around 18–19 months of age). The sustained circulating antibody levels are encouraging particularly in light of recent studies suggesting a decay in neutralization activity in vaccinated[40] and convalescent patients,[41] and support protective efficacy studies in infectious disease challenge models.

The correlates of protection against SARS-CoV-2 in humans have not been clearly defined. While it is well acknowledged that neutralizing antibodies play a critical role, emerging clinical data suggest that the presence of SARS-CoV-2-specific T-cell responses may be an important factor determining COVID-19 severity.[42] Preclinical efficacy studies in mouse models have demonstrated that in the absence of antibodies, T-cell responses can protect against SARS-CoV-2 infection.[43] In addition, recent studies show that the SARS-CoV-2 VOCs can partially escape broadly neutralizing antibody responses but maintain effector and memory T-cell reactivity,[44] further highlighting the complimentary role of T cells in modulating the disease severity for emerging variants. Following vaccination with SCV-S, robust spike-specific polyfunctional CD8 T cells with cytotoxic activity were observed within the first week, which further differentiate to form a memory T-cell pool that can be detected upon secondary stimulation 9 months after vaccination, in both young and middle-aged mice. Notably, spike-specific humoral and cellular immune responses could be detected even in the presence of pre-existing vaccine vector immunity.

Analysis of the antibody repertoire in SARS-CoV-2-recovered individuals revealed the presence of neutralizing antibodies against the S1-NTD and S2 region of the spike protein in addition to anti-RBD antibodies.[45,46] While the exact role and relative contributions of the non-RBD neutralizing antibodies in SARS-CoV-2 infection remain to be fully addressed, it is intuitive to deduce that broad spike-specific antibody responses spanning mutational hotspots (RBD and S1-NTD) and conserved regions (S2) of the spike region, via a combination of anti-S1 and anti-S2 neutralizing antibodies, will offer improved protective efficacy potential against emerging variants. T-cell epitope analysis in naïve individuals revealed reactivity to SARS-CoV-2, with significant proportion of the epitopes mapped to the non-RBD region of the spike protein,[47] suggesting that T-cell responses against the conserved S1-NTD and S2 regions can offer cross-protection against other betacoronaviruses. Our results demonstrate that SCV-S induces a broad spike-specific antibody and CD8 T-cell

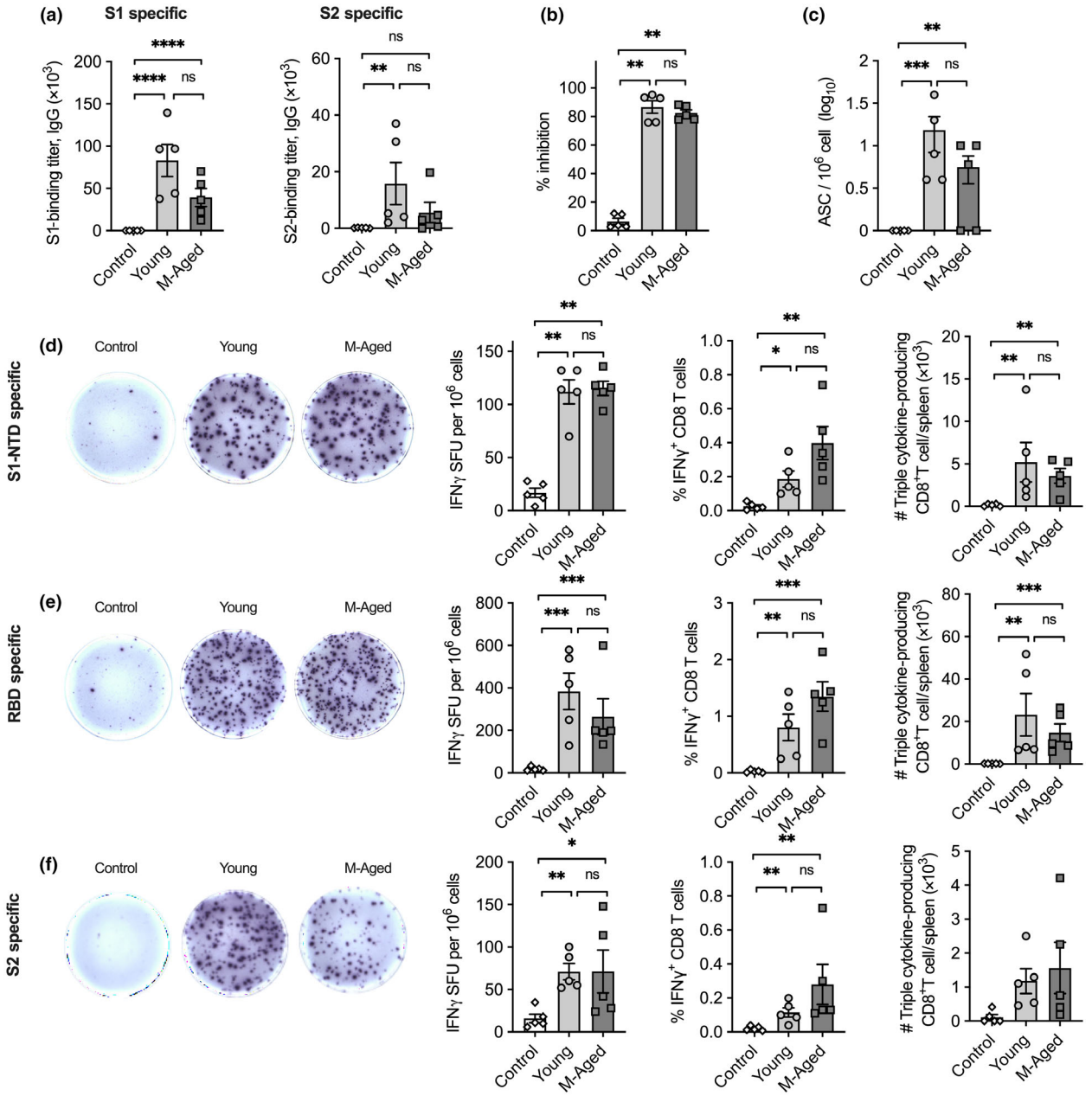

Figure 6. Longevity of spike-specific B- and T-cell responses following SCV-S vaccination. Cohorts of young (6–8 weeks old) and middle-aged (9–10 months old) female C57BL/6J mice ($n = 5$) were vaccinated in a prime-boost regimen (day 0 and 28) with 10^7 PFU of SCV-S or control vector. **(a)** S1-specific (left panel) and S2-specific (right panel) endpoint IgG ELISA titers and **(b)** neutralization titers 9 months after vaccination. **(c)** Frequency of long-lived S1-specific IgG ASCs assessed by B-cell ELISPOT. **(d–f)** Peptide pools (15-amino acid length with 11mer overlaps) spanning the spike protein were used to stimulate splenocytes 9 months after vaccination and IFNγ SFU specific for S1-NTD, RBD and S2 subunit regions of the spike protein was quantitated by ELISPOT (left panels), with frequency of $IFN\gamma^+$ $CD8^+$ T cells (middle panels) and absolute numbers of triple cytokine-producing cells (right panels) enumerated by intracellular cytokine staining and FACS analysis. Symbols represent individual mice and bars show the mean ± s.e.m. from one experiment terminated at this late timepoint. Data were log transformed and statistical significance determined using Brown–Forsythe and Welch ANOVA with Dunnett T3 multiple comparison test. $^*P < 0.05$; $^{**}P < 0.01$; $^{***}P < 0.001$. ASCs, antibody-secreting cells; FACS, fluorescence-activated cell sorting; IFN, interferon; Ig, immunoglobulin; NTD, N-terminal domain; PFU, plaque-forming units; ns, not significant; RBD, receptor-binding domain; SCV-S, Sementis Copenhagen Vector spike protein.

response spanning both the S1 and S2 subunits, enhancing potential activity against other betacoronaviruses and emerging novel SARS-CoV-2 variants.

In summary, while exact replication of each experiment was not performed, the consistency of results from experimental cohorts in independent experiments composed of different genders, inbred and outbred strains and young and middle-aged mice, as well as consistency of antibody and T-cell responses at different timepoints after vaccination, advocates that the SCV-S vaccine induces a rapid, broad, robust and durable spike-specific cellular and humoral response, and thus supports the progression of SCV-based COVID-19 vaccine candidates toward authentic efficacy testing in recognized preclinical SARS-CoV-2 infectious disease challenge trials and clinical development programs. Furthermore, poxvirus-based vectors have a long history as efficient boosters to a wide range of platform technologies such as DNA,[48] protein[49] and viral-vectored platforms.[50] As such, the evidence of serological and cellular priming by the SCV-S vaccine in this study, along with the safety profile of the replication-defective SCV platform, suggests that the vaccine will also be an effective booster to the current vaccines, with potential to enhance spike-specific immune responses. The encouraging immunogenicity profile with a single SARS-CoV-2 antigen also provides impetus to include additional SARS-CoV-2 antigens in second-generation SCV-COVID-19 vaccines, primarily to broaden and strengthen vaccine immunogenicity profiles for enhanced vaccine protective efficacy against current VOCs and new emerging variants as they inevitably become established within the affected global population.

METHODS

Cell lines

The MCL[22] was maintained in CD-CHO media supplemented with 8 mM L-glutamine, penicillin–streptomycin (1 U mL^{-1} and 0.1 mg mL^{-1}, respectively) solution, hygromycin B (500 μg mL^{-1}) and puromycin (10 μg mL^{-1}). 143B cells (ATCC CRL-8303; ATCC, Virginia, USA) were maintained in RPMI-1640 media (Sigma Aldrich, MO, USA) supplemented with 10% fetal bovine serum (Bovogen, VIC, Australia), 2 mM L-glutamine and penicillin–streptomycin. Virus titration was performed in 143B cells expressing D13 (ST01-33) maintained in 143B culture media supplemented with hygromycin B (500 μg mL^{-1}). MC57G cells (ATCC CRL-2295; ATCC, Virginia, USA) were maintained in Eagle's Minimum Essential Medium (Sigma Aldrich, MO, USA) supplemented with 10% fetal bovine serum, 2 mM L-glutamine and penicillin–streptomycin. ACE2-HEK293 recombinant cell line (catalog number 79951; BPS Bioscience, San Diego, CA, USA) was maintained in Dulbecco's Modified Eagle Medium supplemented (Sigma Aldrich, MO, USA) with 10% fetal bovine serum, 2 mM L-glutamine and penicillin–streptomycin. All cell culture reagents were purchased from Thermo Fisher Scientific, Waltham, MA, USA, unless otherwise specified.

Animal experiments

Specific-pathogen-free inbred C57BL/6J and outbred Arc:Arc (S) mice were bred in-house or purchased from the Animal Resources Centre (Canning Vale, WA, Australia). All experiments were conducted under protocols approved by the University of South Australia Animal Ethics Committee in accordance with the *Australian Code for the Care and Use of Animals for Scientific Purposes*, 8th edition (2013). Vaccinations were performed under isoflurane anesthesia by intramuscular administrations into both quadricep muscles of the hind legs.

Construction of SCV-S vaccine

SCV-S vaccine was constructed by replacing the A41L open reading frame with the SARS-CoV-2 spike glycoprotein sequence (21 563–25 384 bp from Wuhan isolate-1; GenBank accession number MN908947). The SARS-CoV-2 spike open reading frame (GeneArt; Thermo Fisher Scientific, Waltham, MA, USA) with a poxvirus early transcriptional stop sequence (T5NT) under the control of a synthetic VACV early/late promoter was cloned into a transfer plasmid containing a comet green fluorescent protein fused with the Zeocin-resistance cassette flanked by a 150-bp repeat sequence, and F1 and F2 arms homologous to upstream and downstream sequences of the *A41L* open reading frame. The resultant transfer plasmid was linearized and transfected into the MCL for homologous recombination with SCV, recombinant VACV in which *D13L*, *B7R/B8R*, *C3L* and *A39R* were previously deleted, at a multiplicity of infection of 0.01. Five rounds of single-cell amplification in the presence of Zeocin was followed by amplification in the absence of Zeocin to delete the fluorescent reporter cassette and generate MVS stocks.

Vaccine stocks and titration

Vaccine stocks were prepared by infecting MCL cells (multiplicity of infection of 0.01) maintained at 33°C, 5% CO_2 in Erlenmeyer flasks shaking at 110 rpm for 48 h. Cell lysis and virus purification were performed as described previously.[22] Vaccine titers were determined by plating serial dilutions on ST01-33 cells incubated at 37°C, 5% CO_2 for 48 h and plaque staining with crystal violet.

In vitro characterization of the SCV-S vaccine

Construction and purity of vaccine stocks were confirmed by PCR (KAPA HiFi polymerase, Roche, Basil, Switzerland) using the primers indicated in Supplementary table 2. PCR products were run on 1% agarose gel and transgene sequence confirmed by Sanger sequencing at the Australian Genome Research Foundation (AGRF Adelaide, SA, Australia).

To assess the genetic stability of SCV-S, serial passages were performed in triplicate. MCL cells (10^6 cells mL^{-1}) were

infected at a multiplicity of infection of 0.01 and harvested 72 h later. Titer was determined by plaque assay to enable the next infection in a similar manner. Genomic DNA (NucleoSpin Tissue kit; Macherey-Nagel, Düren, Germany) for Illumina next-generation sequencing (South Australian Genomics Centre, Adelaide, SA, Australia) was extracted from harvested cultures that were lysed, centrifuged to remove nuclei and cell debris and then incubated with Benzonase (25–50 U mL^{-1}) overnight to degrade host cell DNA. Paired-end reads (150 bp) were mapped to the reference sequence and analyzed using the CLG Genomics Workbench 20 software (Qiagen Digital Insights, CA, USA).

Western blot analysis of spike protein

Cell lysates from 143B cells after 24-h infection with SCV-S or control vector were analyzed by immunoblotting using the SARS-CoV-2 RBD polyclonal antibody (catalog number 40592-T62; Sino Biological, Beijing, China; 1:1000) and anti-rabbit IgG antibody conjugated to horseradish peroxidase (catalog number A9044; Sigma Aldrich, St. Louis, MO, USA; 1:10 000) and imaged using ChemiDoc XRS (Bio-Rad Laboratories, Hercules, CA, USA).

Spike protein expression by flow cytometry

143B cells infected with SCV-S or control vector at a multiplicity of infection of 1, or left uninfected, were harvested at 24 h, stained with live-dead marker (e660 stain; Thermo Fisher Scientific, MA, USA) and anti-SARS-CoV-2 RBD antibody (catalog number 40592-T62; Sino Biological, Beijing, China), followed by staining with phycoerythrin (PE)-conjugated donkey anti-rabbit IgG (catalog number 406421; BioLegend, San Diego, CA, USA). Data were acquired using FACSAria™ Fusion (BD Biosciences, NJ, USA), and analysis performed using FlowJo™ version 10 software (BD Biosciences, NJ, USA).

Plaque immunostaining

Monolayers of ST01-33 in 24-well plates infected with virus were fixed with 1:1 solution of methanol/ acetone and immunostained with rabbit SARS-CoV-2 RBD antibody (catalog number 40592-T62; Sino Biological, Beijing, USA) and horseradish peroxidase-conjugated anti-rabbit IgG antibody (Life Technologies, Carlsbad, CA, USA).

IFNγ ELISPOT assay

ELISPOT plates (MSIPS4510; Millipore, Burlington, MA, USA) were activated, washed, coated with anti-mouse IFNγ capture antibody (clone AN18; Thermo Fisher Scientific, MA, USA; 8 μg mL^{-1}) and incubated overnight at 4°C. The next day, serial dilutions of splenocytes were added to blocked ELISPOT plates and stimulated with 2 μg mL^{-1} of each peptide for 18 h. Plates were washed, incubated with biotinylated anti-mouse IFNγ antibody (clone R4-6A2; Mabtech, Stockholm, Sweden; 1 μg mL^{-1}) followed by treatment with streptavidin–alkaline phosphatase (catalog number 3310-10; Mabtech, Stockholm, Sweden). Spots were visualized using BCIP/NBT plus substrate (catalog number 3650-10; Mabtech, Stockholm, Sweden) and counted using an automated ELISPOT plate reader (AID vSpot Spectrum; Autoimmun Diagnostika GMBH, Strassberg, Germany).

Cytotoxic T-lymphocyte assay

MC57G target cells were pulsed with 2 μg mL^{-1} of peptide, radiolabeled and incubated with effector splenocytes for 6 h at an effector-to-target cell ratio of 100:1. Maximum and spontaneous release controls were set up for each condition. Luma plate (PerkinElmer, MA, USA) were coated with 30 μL of the supernatant, allowed to dry overnight and counts recorded on a top count MicroBeta plate reader. Percent specific lysis was calculated using the following equation: [(sample ^{51}Cr release − spontaneous ^{51}Cr release)/(maximum ^{51}Cr release − spontaneous ^{51}Cr release)] × 100.

T-cell analysis by flow cytometry

Intracellular cytokine staining was performed by stimulating splenocytes with 2 μg mL^{-1} per peptide for 2 h followed by the addition of brefeldin A (final concentration 10 μg mL^{-1}) and incubation for additional 4 h. Cells were surface stained for 30 min at 4°C with anti-mouse CD3 APC-CY7 (clone 17A2), anti-mouse CD4 BV510 (clone RM4-5) and anti-mouse CD8a PE (clone 53-6.7) followed by staining with LIVE/DEAD fixable e660 stain. Cell were fixed and permeabilized using Cytofix/Cytoperm kit (BD Biosciences) as per the manufacturer's instructions, followed by staining with anti-mouse IFNγ fluorescein isothiocyanate (clone XMG1.1), anti-mouse TNF-α BV421 (clone MP6-XT22), anti-mouse IL-2 PE-CF594 (clone JES-5H4) and anti-human/mouse granzyme B PE-Cy7 (clone Q1A6A02; BioLegend, CA, USA) overnight. All antibodies were purchased from BD Biosciences, NJ, USA unless mentioned otherwise. Data were acquired on FACSAria™ Fusion and analyzed by FlowJo™ V10 software.

Memory T-cell populations were identified by surface staining with the following anti-mouse antibodies: CD3 APC-CY7 (clone 17A2), CD4 BV510 (clone RM4-5), CD8a PE (clone 53-6.7), CD44 fluorescein isothiocyanate (clone IM7), KLRG1 PE-CF594 (clone 2F1), CD62L BV650 (clone MEL-14) and CD127 BV421 (clone A7R34).

Binding antibody titers

High-binding 96-well plates (Nunc, Thermo Fisher Scientific, MA, USA) were coated with the antigen (S1 protein 1.2 μg mL^{-1}; S2 0.8 μg mL^{-1}; SCV 10^5 plaque-forming units/well) in carbonate buffer (pH 9.8) and incubated at 4°C overnight. Plates were washed, blocked and incubated with serial dilutions of serum in 1% skim milk powder for 2 h at room temperature. Binding antibodies were detected using horseradish peroxidase-conjugated anti-mouse IgG (catalog number A9044; Sigma Aldrich, St. Louis, MO, USA), IgG1 (catalog number 1070-05; Southern Biotech, AL, USA), IgG2b (catalog number 1090-05; Southern Biotech, AL, USA), IgG2c

(catalog number 1079-05; Southern Biotech, AL, USA), IgG3 (catalog number 11100-05; Southern Biotech, AL, USA) and signals developed using 3,3′,5,5′-tetramethylbenzidine substrate (catalog number T0440; Sigma-Aldrich, St. Louis, MO, USA). Endpoint titers were defined as the highest reciprocal of serum dilution to yield an absorbance equal to the negative serum samples plus three times the standard deviation.

SARS-CoV-2 neutralization antibody detection

Neutralizing activity was determined using the cPass SARS-CoV-2 neutralization antibody detection kit (GenScript, Piscataway, NJ, USA) as per the manufacturer's instructions. Serum samples and controls were incubated with horseradish peroxidase-conjugated RBD, transferred to an ACE2-coated capture plate and signal developed using the 3,3′,5,5′-tetramethylbenzidine substrate. Percent inhibition determined as follows: (1 − OD value of sample/OD value of negative control) × 100%, where OD is the optical density reading at 450 nm.

Lentivirus-based pseudovirus neutralization assay

Neutralizing activity against SARS-CoV-2 variants was examined using spike-pseudotyped lentiviruses in ACE2-HEK293 recombinant cell line and quantitated as reductions in luciferase reporter expression as per the manufacturer's instructions (BPS Bioscience, CA, USA). Original SARS-CoV-2 spike-pseudotyped lentivirus (catalog number 79442; BPS Bioscience, CA, USA), spike B.1.1.7 (alpha) variant-pseudotyped lentivirus (catalog number 78112; BPS Bioscience, CA, USA) and spike B.1.351 (beta) variant-pseudotyped lentivirus (catalog number 78142; BPS Bioscience, CA, USA) were used. The 80% inhibitory concentration titers were determined using a log (inhibitor) *versus* normalized-response (variable slope) nonlinear regression model in Prism version 9 (GraphPad Software, CA, USA).

Antibody-secreting cell ELISPOT

ELISPOT plates (MSIPS4510; Millipore, MA, USA) were activated, washed, coated with S1 protein (10 μg mL^{-1}) and incubated overnight at 4°C. The next day, bone marrow cells (5×10^6 cells) were added to blocked ELISPOT plates and incubated for 24 h. Plates were washed, incubated with biotinylated anti-IgG detection antibody (catalog number 3826-5; Mabtech, Stockholm, Sweden; 1 μg mL^{-1}) and treated with streptavidin–alkaline phosphatase (catalog number 3310-10, Mabtech, Stockholm, Sweden; 1:1000). Spots were visualized using BCIP/NBT plus substrate (catalog number 3650-10, Mabtech, Stockholm, Sweden) and counted using an ELISPOT plate reader (AID vSpot Spectrum; Autoimmun Diagnostika GMBH, Strassberg, Germany).

Statistics

GraphPad Prism version 9.0 (GraphPad software, CA, USA) was used for statistical analysis. Data were log-transformed and where appropriate Brown–Forsythe and Welch ANOVA with Dunnett T3 multiple comparison test for unpaired samples or repeated-measures ANOVA with Tukey multiple comparison test for paired samples was used to determine statistical significance between three or more group. For statistical analysis between two groups, *t*-tests with Welch's correction was used. Correlation analysis was performed using the Spearman rank test.

ACKNOWLEDGMENTS

The authors acknowledge the contributions of Paul M Howley, past CEO/CSO of Sementis Ltd, and Robyn Kievit for technical support to this work, as well as The University of Queensland Protein Expression Facility and GenScript for providing reagents and additional support. Open access publishing facilitated by University of South Australia, as part of the Wiley–University of South Australia agreement via the Council of Australian University Librarians.

CONFLICT OF INTEREST

The authors declare the following competing interests: RGG, PW, LH and JH are current or past employees of Sementis Limited. PE, TC, NP, LL, KD and JH are named on a PCT patent application covering SCV-COVID19 vaccines (applicant: Sementis Limited; application number: PCT/AU2021/050274). PE, TC, NP, LL, GH, JZ, RGG, PW, LH, KD and JH own stock or hold stock options. This research was conducted as a collaboration between UniSA and Sementis Ltd, with UniSA salaries and project support from funds provided by Sementis Ltd. AT declares no competing interests.

AUTHOR CONTRIBUTIONS

Preethi Eldi: Conceptualization; Formal analysis; Investigation; Methodology; Writing—original draft; Writing—review and editing. **Tamara H Cooper:** Conceptualization; Investigation; Writing—review and editing. **Natalie A Prow:** Conceptualization; Investigation; Writing—review and editing. **Liang Liu:** Conceptualization; Methodology. **Gary K Heinemann:** Investigation; Writing—review and editing. **Voueleng J Zhang:** Investigation; Writing—review and editing. **Abigail D Trinidad:** Investigation. **Ruth Marian Guzman-Genuino:** Conceptualization. **Peter Wulff:** Conceptualization. **Leanne M Hobbs:** Conceptualization; Funding acquisition; Writing—original draft; Writing—review and editing. **Kerrilyn R Diener:** Conceptualization; Project administration; Visualization; Writing—original draft; Writing—review and editing. **John D Hayball:** Conceptualization; Supervision; Writing—original draft; Writing—review and editing.

DATA AVAILABILITY STATEMENT

All data sets generated and analyzed in the current research are available from the corresponding authors upon reasonable request.

REFERENCES

1. Zhu N, Zhang D, Wang W, *et al.* A novel Coronavirus from patients with pneumonia in China, 2019. *N Engl J Med* 2020; **382**: 727–733.
2. WHO Coronavirus (COVID-19) dashboard. https://covid19whoint/2021
3. Fang L, Karakiulakis G, Roth M. Are patients with hypertension and diabetes mellitus at increased risk for COVID-19 infection? *Lancet Respir Med* 2020; **8**: e21.
4. Li B, Yang J, Zhao F, *et al.* Prevalence and impact of cardiovascular metabolic diseases on COVID-19 in China. *Clin Res Cardiol* 2020; **109**: 531–538.
5. Lighter J, Phillips M, Hochman S, *et al.* Obesity in patients younger than 60 years is a risk factor for COVID-19 hospital admission. *Clin Infect Dis* 2020; **71**: 896–897.
6. Suarez-Garcia I, Perales-Fraile I, Gonzalez-Garcia A, *et al.* In-hospital mortality among immunosuppressed patients with COVID-19: Analysis from a national cohort in Spain. *PLoS One* 2021; **16**: e0255524.
7. Davies NG, Abbott S, Barnard RC, *et al.* Estimated transmissibility and impact of SARS-CoV-2 lineage B.1.1.7 in England. *Science* 2021; **372**: eabg3055.
8. Tegally H, Wilkinson E, Giovanetti M, *et al.* Detection of a SARS-CoV-2 variant of concern in South Africa. *Nature* 2021; **592**: 438–443.
9. Faria NR, Mellan TA, Whittaker C, *et al.* Genomics and epidemiology of the P.1 SARS-CoV-2 lineage in Manaus, Brazil. *Science* 2021; **372**: 815–821.
10. Yadav PD, Sapkal GN, Abraham P, *et al.* Neutralization of variant under investigation B.1.617 with sera of BBV152 vaccinees. *Clin Infect Dis* 2021; **74**: 366–368.
11. Mlcochova P, Kemp S, Dhar MS, *et al.* SARS-CoV-2 B.1.617.2 Delta variant replication and immune evasion. *Nature* 2021; **599**: 114–119.
12. Polack FP, Thomas SJ, Kitchin N, *et al.* Safety and efficacy of the BNT162b2 mRNA Covid-19 vaccine. *N Engl J Med* 2020; **383**: 2603–2615.
13. Baden LR, El Sahly HM, Essink B, *et al.* Efficacy and safety of the mRNA-1273 SARS-CoV-2 vaccine. *N Engl J Med* 2021; **384**: 403–416.
14. Voysey M, Clemens SAC, Madhi SA, *et al.* Safety and efficacy of the ChAdOx1 nCoV-19 vaccine (AZD1222) against SARS-CoV-2: an interim analysis of four randomised controlled trials in Brazil, South Africa, and the UK. *Lancet* 2021; **397**: 99–111.
15. Sadoff J, Gray G, Vandebosch A, *et al.* Safety and efficacy of single-dose Ad26.COV2.S vaccine against Covid-19. *N Engl J Med* 2021; **384**: 2187–2201.
16. Tscherne A, Schwarz JH, Rohde C, *et al.* Immunogenicity and efficacy of the COVID-19 candidate vector vaccine MVA-SARS-2-S in preclinical vaccination. *Proc Natl Acad Sci USA* 2021; **118**: e2026207118.
17. Lu M, Dravid P, Zhang Y, *et al.* A safe and highly efficacious measles virus-based vaccine expressing SARS-CoV-2 stabilized prefusion spike. *Proc Natl Acad Sci USA* 2021; **118**: e2026153118.
18. Malherbe DC, Kurup D, Wirblich C, *et al.* A single dose of replication-competent VSV-vectored vaccine expressing SARS-CoV-2 S1 protects against virus replication in a hamster model of severe COVID-19. *NPJ Vaccines* 2021; **6**: 91.
19. Ella R, Reddy S, Jogdand H, *et al.* Safety and immunogenicity of an inactivated SARS-CoV-2 vaccine, BBV152: interim results from a double-blind, randomised, multicentre, phase 2 trial, and 3-month follow-up of a double-blind, randomised phase 1 trial. *Lancet Infect Dis* 2021; **21**: 950–961.
20. Tanriover MD, Doganay HL, Akova M, *et al.* Efficacy and safety of an inactivated whole-virion SARS-CoV-2 vaccine (CoronaVac): interim results of a double-blind, randomised, placebo-controlled, phase 3 trial in Turkey. *Lancet* 2021; **398**: 213–222.
21. Heath PT, Galiza EP, Baxter DN, *et al.* Safety and efficacy of NVX-CoV2373 Covid-19 vaccine. *N Engl J Med* 2021; **385**: 1172–1183.
22. Eldi P, Cooper TH, Liu L, *et al.* Production of a Chikungunya vaccine using a CHO Cell and attenuated viral-based platform technology. *Mol Ther* 2017; **25**: 2332–2344.
23. Zhang Y, Moss B. Immature viral envelope formation is interrupted at the same stage by lac operator-mediated repression of the vaccinia virus D13L gene and by the drug rifampicin. *Virology* 1992; **187**: 643–653.
24. Liu L, Cooper T, Howley PM, Hayball JD. From crescent to mature virion: vaccinia virus assembly and maturation. *Viruses* 2014; **6**: 3787–3808.
25. Prow NA, Liu L, Nakayama E, *et al.* A vaccinia-based single vector construct multi-pathogen vaccine protects against both Zika and chikungunya viruses. *Nat Commun* 2018; **9**: 1230.
26. Hazlewood JE, Dumenil T, Le TT, *et al.* Injection site vaccinology of a recombinant vaccinia-based vector reveals diverse innate immune signatures. *PLoS Pathog* 2021; **17**: e1009215.
27. Prow NA, Liu L, McCarthy MK, *et al.* The vaccinia virus based Sementis Copenhagen Vector vaccine against Zika and chikungunya is immunogenic in non-human primates. *NPJ Vaccines* 2020; **5**: 44.
28. Chakrabarti S, Sisler JR, Moss B. Compact, synthetic, vaccinia virus early/late promoter for protein expression. *Biotechniques* 1997; **23**: 1094–1097.
29. Jenne DE, Tschopp J. Granzymes, a family of serine proteases released from granules of cytolytic T lymphocytes upon T cell receptor stimulation. *Immunol Rev* 1988; **103**: 53–71.
30. Boyd A, Almeida JR, Darrah PA, *et al.* Pathogen-specific T cell polyfunctionality is a correlate of T cell efficacy and immune protection. *PLoS One* 2015; **10**: e0128714.
31. Cui W, Kaech SM. Generation of effector $CD8^+$ T cells and their conversion to memory T cells. *Immunol Rev* 2010; **236**: 151–166.
32. World Health organisation R&D Blue print. WHO Target Product Profiles for COVID-19 Vaccines; 2020. https://www.who.int/publications/m/item/who-target-product-profiles-for-covid-19-vaccines

33. Bolles M, Deming D, Long K, *et al.* A double-inactivated severe acute respiratory syndrome coronavirus vaccine provides incomplete protection in mice and induces increased eosinophilic proinflammatory pulmonary response upon challenge. *J Virol* 2011; **85**: 12201–12215.
34. Tseng CT, Sbrana E, Iwata-Yoshikawa N, *et al.* Immunization with SARS coronavirus vaccines leads to pulmonary immunopathology on challenge with the SARS virus. *PLoS One* 2012; **7**: e35421.
35. Henry C, Zheng NY, Huang M, *et al.* Influenza virus vaccination elicits poorly adapted B cell responses in elderly individuals. *Cell Host Microbe* 2019; **25**: e356.
36. Grubeck-Loebenstein B. Fading immune protection in old age: vaccination in the elderly. *J Comp Pathol* 2010; **142** (Suppl 1): S116–119.
37. Slifka MK, Matloubian M, Ahmed R. Bone marrow is a major site of long-term antibody production after acute viral infection. *J Virol* 1995; **69**: 1895–1902.
38. Halliley JL, Tipton CM, Liesveld J, *et al.* Long-lived plasma cells are contained within the $CD19^{-}CD38^{hi}CD138^{+}$ subset in human bone marrow. *Immunity* 2015; **43**: 132–145.
39. Taylor SC, Hurst B, Charlton CL, *et al.* A New SARS-CoV-2 dual-purpose serology test: highly accurate infection tracing and neutralizing antibody response detection. *J Clin Microbiol* 2021; **59**: e02438–e2520.
40. Wei J, Stoesser N, Matthews PC, *et al.* Antibody responses to SARS-CoV-2 vaccines in 45,965 adults from the general population of the United Kingdom. *Nat Microbiol* 2021; **6**: 1140–1149.
41. Khoury DS, Cromer D, Reynaldi A, *et al.* Neutralizing antibody levels are highly predictive of immune protection from symptomatic SARS-CoV-2 infection. *Nat Med* 2021; **27**: 1205–1211.
42. Sekine T, Perez-Potti A, Rivera-Ballesteros O, *et al.* Robust T cell immunity in convalescent individuals with asymptomatic or mild COVID-19. *Cell* 2020; **183**(158–168): e114.
43. Zhuang Z, Lai X, Sun J, *et al.* Mapping and role of T cell response in SARS-CoV-2-infected mice. *J Exp Med* 2021; **218**: e20202187.
44. Tarke A, Sidney J, Methot N, *et al.* Impact of SARS-CoV-2 variants on the total $CD4^{+}$ and $CD8^{+}$ T cell reactivity in infected or vaccinated individuals. *Cell Rep Med* 2021; **2**: 100355.
45. Huang KA, Tan TK, Chen TH, *et al.* Breadth and function of antibody response to acute SARS-CoV-2 infection in humans. *PLoS Pathog* 2021; **17**: e1009352.
46. Zheng Z, Monteil VM, Maurer-Stroh S, *et al.* Monoclonal antibodies for the S2 subunit of spike of SARS-CoV-1 cross-react with the newly-emerged SARS-CoV-2. *Euro Surveill* 2020; **25**: 2000291.
47. Mateus J, Grifoni A, Tarke A, *et al.* Selective and cross-reactive SARS-CoV-2 T cell epitopes in unexposed humans. *Science* 2020; **370**: 89–94.
48. Viegas EO, Kroidl A, Munseri PJ, *et al.* Optimizing the immunogenicity of HIV prime-boost DNA-MVA-rgp140/GLA vaccines in a phase II randomized factorial trial design. *PLoS One* 2018; **13**: e0206838.
49. Shen X, Basu R, Sawant S, *et al.* HIV-1 gp120 and Modified Vaccinia Virus Ankara (MVA) gp140 Boost Immunogens Increase Immunogenicity of a DNA/MVA HIV-1 Vaccine. *J Virol* 2017; **91**: e01077–17.
50. Pollard AJ, Launay O, Lelievre JD, *et al.* Safety and immunogenicity of a two-dose heterologous Ad26.ZEBOV and MVA-BN-Filo Ebola vaccine regimen in adults in Europe (EBOVAC2): a randomised, observer-blind, participant-blind, placebo-controlled, phase 2 trial. *Lancet Infect Dis* 2021; **21**: 493–506.

SUPPORTING INFORMATION

Additional supporting information may be found online in the Supporting Information section at the end of the article.